European Radiology (2019) 29:392–400
https://doi.org/10.1007/s00330-018-5581-1

GASTROINTESTINAL

Radiomics nomogram outperforms size criteria in discriminating lymph node metastasis in resectable esophageal squamous cell carcinoma

Xianzheng Tan[1,2,3] · Zelan Ma[4] · Lifen Yan[1,2] · Weitao Ye[2] · Zaiyi Liu[1,2] · Changhong Liang[1,2]

Received: 28 February 2018 / Revised: 23 May 2018 / Accepted: 1 June 2018 / Published online: 19 June 2018

Abstract

Objectives To determine the value of radiomics in predicting lymph node (LN) metastasis in resectable esophageal squamous cell carcinoma (ESCC) patients.

Methods Data of 230 consecutive patients were retrospectively analyzed (154 in the training set and 76 in the test set). A total of 1576 radiomics features were extracted from arterial-phase CT images of the whole primary tumor. LASSO logistic regression was performed to choose the key features and construct a radiomics signature. A radiomics nomogram incorporating this signature was developed on the basis of multivariable analysis in the training set. Nomogram performance was determined and validated with respect to its discrimination, calibration and reclassification. Clinical usefulness was estimated by decision curve analysis.

Results The radiomics signature including five features was significantly associated with LN metastasis. The radiomics nomogram, which incorporated the signature and CT-reported LN status (i.e. size criteria), distinguished LN metastasis with an area under curve (AUC) of 0.758 in the training set, and performance was similar in the test set (AUC 0.773). Discrimination of the radiomics nomogram exceeded that of size criteria alone in both the training set (p <0.001) and the test set (p=0.005). Integrated discrimination improvement (IDI) and categorical net reclassification improvement (NRI) showed significant improvement in prognostic value when the radiomics signature was added to size criteria in the test set (IDI 17.3%; p<0.001; categorical NRI 52.3%; p<0.001). Decision curve analysis supported that the radiomics nomogram is superior to size criteria.

Conclusions The radiomics nomogram provides individualized risk estimation of LN metastasis in ESCC patients and outperforms size criteria.

Key Points

- *A radiomics nomogram was built and validated to predict LN metastasis in resectable ESCC.*
- *The radiomics nomogram outperformed size criteria.*
- *Radiomics helps to unravel intratumor heterogeneity and can serve as a novel biomarker for determination of LN status in resectable ESCC.*

Keywords Esophageal squamous cell carcinoma · Lymphatic metastasis · Diagnostic imaging · Nomograms · Precision medicine

Electronic supplementary material The online version of this article (https://doi.org/10.1007/s00330-018-5581-1) contains supplementary material, which is available to authorized users.

✉ Zaiyi Liu
zyliu@163.com

✉ Changhong Liang
cjr.lchh@vip.163.com

[1] The Second School of Clinical Medicine, Southern Medical University, Guangzhou 510515, People's Republic of China

[2] Department of Radiology, Guangdong General Hospital, Guangdong Academy of Medical Sciences, 106 Zhongshan Er Road, Guangzhou 510080, Guangdong, People's Republic of China

[3] Department of Radiology, Hunan Provincial People's Hospital, Changsha 410005, Hunan Province, People's Republic of China

[4] Guangdong Provincial Traditional Chinese Medicine Hospital, Guangzhou, Guangdong Province 510120, People's Republic of China

Abbreviations

AJCC	American Joint Committee on Cancer
AUC	Area under curve
CT	Computed tomography
ESCC	Esophageal squamous cell carcinoma
GLCM	Gray level co-occurrence matrix
GLRLM	Gray level run length matrix
GLSZM	Gray level size zone matrix
ICC	Intra-class correlation coefficient
IDI	Integrated discrimination improvement
LASSO	Least absolute shrinkage and selection operator
LN	Lymph node
NLR	Neutrophil-to-lymphocyte ratio
NRI	Net reclassification improvement
PLR	Platelet-to-lymphocyte ratio
ROC	Receiver operator characteristic
VOI	Volume of interest

Introduction

Esophageal carcinoma is the eleventh most common cancer and the sixth leading cause of cancer mortality globally [1]. An estimated 455,800 new esophageal cancer cases and 400,200 deaths occurred in 2012 worldwide [2]. Esophageal squamous cell carcinoma (ESCC) is the predominant histological subtype. In high-risk areas such as China, ESSC accounts for more than 90% of all esophageal carcinoma cases [3, 4].

Lymph node (LN) metastasis is the most important prognostic factor in esophageal cancer, with a rising number of metastatic lymph nodes heralding worse disease outcome [5, 6]. Accurate preoperative diagnosis of LN metastasis in patients with ESCC is crucial for decision making and pretreatment prognostication [7]. Important findings were that preoperative identification of LN metastasis, currently based mainly on radiological modalities, remains inaccurate and coarse [8–10]. The reported accuracy of computed tomography (CT) in the detection of LN metastasis in esophageal cancer on the basis of a short-axis diameter of 10 mm is just 46% to 58% [7, 9, 10]. The inability to accurately determine LN metastasis may result in inappropriate treatment.

Recent advances in radiomics enable the noninvasive decoding of tumor heterogeneity [11–15]. It has been reported that a radiomics nomogram can enable superior prediction of LN metastasis in colorectal cancer and bladder cancer [16, 17]. To our knowledge, there is no published study on the accuracy of radiomics for detecting pathological LN metastasis in ESCC and no study on the comparison of radiomics and traditional metrics such as LN size.

Therefore, the primary objective of this study was to assess the ability of radiomics in predicting regional LN metastasis in ESCC. The secondary objective was to investigate its incremental value to conventional metrics.

Materials and methods

Patients

An institutional review board waiver was obtained for this retrospective study. Patients who underwent radical esophagostomy and regional lymphadenectomy between January 2012 and September 2016 were identified from the institutional database. Inclusion criteria were: (a) patients who underwent radical esophagostomy with extensive LN dissection in two or three fields; (b) histologically confirmed ESCC; (c) standard contrast-enhanced CT performed less than two weeks before surgical resection. Exclusion criteria included: (a) preoperative neoadjuvant chemotherapy or radiation therapy (n=156); (b) esophageal multiple primary carcinoma or concurrence squamous cell cancer (n=55); (c) uninterpretable enhanced CT images (n=7); (d) poor visualization of the tumor due to too small size (n=11); (e) incomplete clinical information (n=17). Two hundred thirty patients who met the criteria were divided randomly into training set (n=154) and test set (n=76) in a 2:1 ratio. The patient recruitment pathway is shown in Supplementary Fig. S1.

Baseline clinical and histopathological data were derived from medical records. Preoperative blood-routine characteristics (within two weeks before surgery) including neutrophil, lymphocyte and platelet count were collected to calculated neutrophil-to-lymphocyte ratio (NLR) and platelet-to-lymphocyte ratio (PLR). Tumor location was defined by epicenter of esophageal tumor according to the 8th edition of the American Joint Committee on Cancer (AJCC) Cancer Staging Manual, which is determined from chest CT images [18, 19]. CT-reported LN status was assessed on the pretreatment CT by a radiologist who had 15 years of experience (largely with esophageal cancer). The short axis diameter of the largest regional LN >10mm was defined as a radiological positive nodal status [7]. The pathological LN status of each case was identified according to the histopathological reports.

CT imaging protocol

All patients underwent contrast-enhanced imaging with a 64-slice LightSpeed VCT (GE Healthcare). Examinations were performed during a single breath-hold with the patient supine. The scanning coverage was from sternal notch to the middle of the kidneys. The CT parameters were as follows: 120 kVp; 130-280 mAs; 0.4s rotation time; detector collimation 64 ×0.625 mm; field of view (FOV) 300-400mm; matrix 512 × 512. After routine non-enhanced CT, arterial phase contrast-enhanced CT was started 25–30 s after an intravenous

administration of 1.5 ml/kg of the iodinated contrast material (Ultravist 370, Bayer Schering Pharma) at a rate of 3.0 to 3.5 mL/s via a pump injector (Ulrich CT Plus 150, Ulrich Medical). The administration of the contrast medium was followed by a saline flush. The raw data were reconstructed with 5.0-mm section thickness.

Radiomics workflow

Radiomics workflow is illustrated in Fig. 1, including (1) tumor segmentation, (2) radiomics feature extraction, (3) feature selection and predictive classifier development (described in Statistical Analysis in detail).

Tumor segmentation

Arterial-phase CT images were retrieved from PACS (Carestream) for tumor segmentation because the arterial phase was the optimal one for visualization of esophageal cancer [20]. The visible tumors were manually segmented slice by slice using the open source software 3D Slicer (version 4.6, http://www.slicer.org). A thoracic radiologist with 8 years of experience in esophageal imaging, who was blinded to the clinicopathological data but was aware that the patients had ESCC, independently placed the volume of interest (VOI). The lesion was determined to be cancerous when the esophageal wall showed focal thickening of ≥5 mm on transverse imaging. The VOIs were delineated around the tumor outline. Intraluminal air, oral contrast material and tumor necrosis adjacent to lumen were excluded. Besides, periesophageal fat, visually identified blood vessels adjacent to the tumor should not be involved. This process was further refined with a thresholding procedure that excluded any pixels with attenuation values below -50 HU and beyond 300 HU. To evaluate the reproducibility of the radiomics analysis, tumor segmentation was repeated two months later by the same observer for 30 randomly chosen patients.

Radiomics feature extraction

The calculation of all features was implemented with PyRadiomics toolbox in Python 3.6.2 (https://www.python.org), an open-source python package for the extraction of radiomics features from medical imaging [21]. Ninety-four radiomics features were extracted from the original images including 19 first order features, 16 shape features and 59 texture features derived from gray level co-occurrence matrix (GLCM) , gray level size zone matrix (GLSZM) , and gray level run length matrix (GLRLM) . By applying a Laplacian of Gaussian filter with three sigma levels (1.0, 2.0, 3.0), 234 features were obtained. By using “haar” and “dmey” wavelet decomposition, eight derived images were yielded and 1248 wavelet features generated. In total, 1576 individual features were extracted. Feature descriptions and mathematical definitions can be found elsewhere (see: http://pyradiomics.readthedocs.io/en/latest/features.html).

Statistical analysis

Statistical analyses were performed on R software (version 3.4.0, https://www.r-project.org). A p value of 0.05 was considered as statistical significance using two-sided testing.

Demographic comparison between training set and test set

An independent samples t-test or Mann-Whitney U test, where appropriate, was used to assess the differences in age, NLR and PLR between the training set and test set, while chi-squared tests were used to compare the differences in categorical variables (gender, tumor location, CT-reported LN status, pathological LN status).

Intra-observers reproducibility of radiomics features

The intra-class correlation coefficient (ICC) was calculated to estimate intra-reader agreement of each radiomics feature.

Features selection and radiomic signature building

To prioritize the high-dimensional features, only the features with ICCs value≥0.900 were firstly selected on the basis of reproducibility. Then, the stable features were entered into the least absolute shrinkage and selection operator (LASSO) logistic regression model to identify the optimal features in the training set.

To better evaluate the performance of the optimal radiomics features in predicting LN metastasis, a radiomics score (Rad-score) was calculated for each patient, with the coefficients weighted by LASSO logistic regression model in the training set. The difference in Rad-score between the training set and test set was assessed by using the samples t-test. Univariable association analysis between the Rad-score and LN status was first assessed in the training set and then validated in the test set.

Development of the radiomics nomogram

Multivariable logistic regression analysis started with the following candidate variables: age, gender, tumor location, NLR, PLR, CT-reported LN status and Rad-score. Backward stepwise selection was used with a significance level of 0.05 for variable retention. To develop a clinically applicable tool that could predict an individual’s LN metastasis probability, we

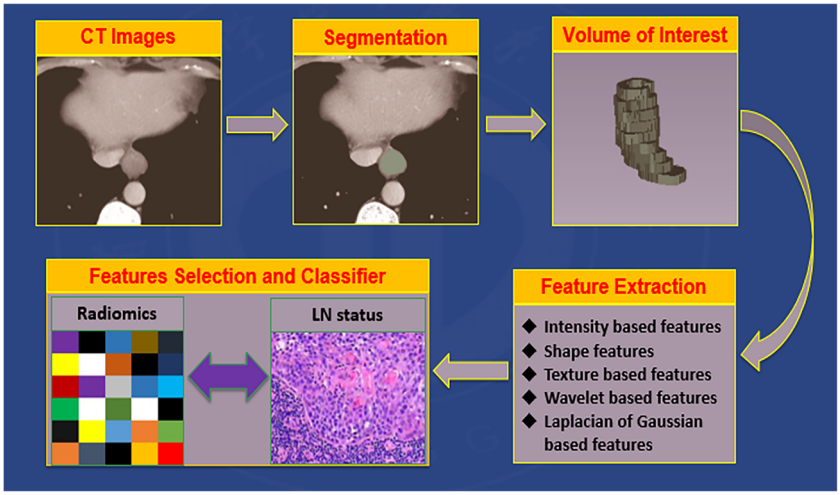

Fig. 1 The process of radiomics

generated a nomogram on the basis of the multivariate analysis in the training set.

Prediction performance of the nomogram

The performance of the radiomics nomogram was first evaluated in the training set and then validated in the test set with respect to its calibration, discrimination, and reclassification. Calibration was assessed by Hosmer-Lemeshow test. Radiomics nomogram discrimination was quantified by area under curve (AUC). The differences in the AUCs between CT-reported LN status and the radiomics nomogram were compared using the Delong test. The additional diagnostic value of radiomics signature to CT-reported LN status was evaluated by using integrated discrimination improvement (IDI) and categorical net reclassification improvement (NRI) indexes. Decision curve analysis was used to determine the clinical impact of the radiomics nomogram.

Influence of interobserver variability on the nomogram

In the course of building a nomogram, only one observer was chosen to determine CT-reported LN status or delineate VOI. To explore the potential impact of multiple observers on the radiomics nomogram, we assessed the interobserver reproducibility of CT-reported LN status and optimal radiomics features, with the corresponding methods and results provided in Supplementary S1.

Results

Patient characteristics

The details of patient characteristics in the training set and test set are presented in Fig. 2 and Supplementary Table S1. LN metastasis positivities in the training set and test set were 52.6% and 48.7%, respectively. That there were no significant differences in clinicopathological characteristics between the two data sets justified their use as training set and test set (p = 0.302-1.000 [see Supplementary Table S1]).

Selection of candidate radiomics features and building a radiomics signature

Before features selection, 1576 extracted radiomics features were normalized with z-score method. Using the filter criteria of ICCs≥0.900, we derived a list of 1338 features (ICC range: 0.900-1.000) with 238 features eliminated (ICC range: 0.373-0.899). Next, we used the LASSO algorithm to select the most significant radiomics features for classifying LN metastasis (-) and LN metastasis (+) patients in the training set (Fig. 3). As a

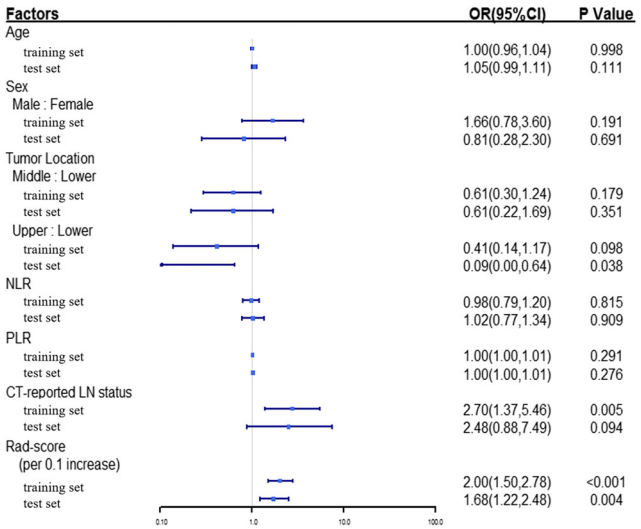

Fig. 2 Association of clinical characteristics and pathological LN status in the training set and test set. Abbreviations: OR, Odds Ratio; 95% CI, 95% confidence interval; NLR, neutrophil to lymphocyte ratio; PLR, platelet count to lymphocyte ratio; CT, computed tomography; LN, lymph node

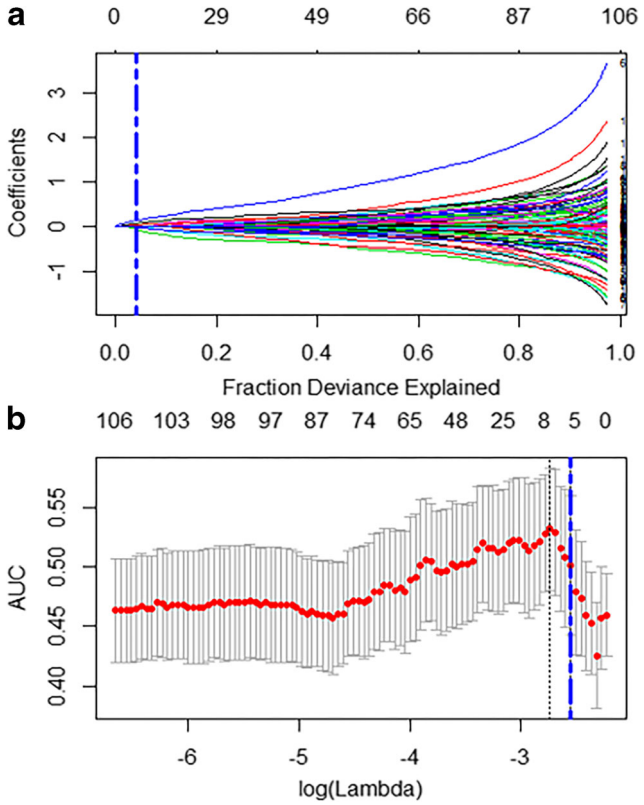

Fig. 3 Selection of lymph node metastasis-associated radiomics features via least absolute shrinkage and selection operator (LASSO) algorithm. Top figure (**a**) shows the coefficient profiles of 1338 radiomics features against the deviance explained, bottom figure (**b**) the cross-validation curve. Blue dotted vertical lines were drawn at the optimal value by using 10-fold cross-validation and the 1 standard error of the minimum criteria (the 1-SE criteria). An optimal lambda value of 0.0779, with log (lambda) = -2.5523, was selected, and 5 nonzero coefficients were chosen

result, five features were identified, including original_glszm_GrayLevelVariance, log.sigma.1.mm.3D_glrlm_RunVariance, wavelet.haar.LHH_glszm_GrayLevelNonUniformity, wavelet.dmey.LHH_glcm_Imc1 and wavelet.dmey.LHL_firstorder_Kurtosis. The Rad-score was calculated as follows: *Rad-score =0.10486682 - (0.06509694 × original_glszm_GrayLevelVariance) + (0.03504278 × log.sigma.1.mm.3D_glrlm_RunVariance) + (0.13552659 × wavelet.haar.LHH_glszm_GrayLevelNonUniformity) + (0.05970465 × wavelet.dmey.LHH_glcm_Imc1) - (0.02165378 × wavelet.dmey.LHL_firstorder_Kurtosis).*

Validating the radiomics signature

Significant association between the Rad-score and pathological LN status was found in the training set (Odds Ratio [OR] 2.00; 95% CI 1.50 to 2.78; $p<0.001$; Fig. 2) and then confirmed in the test set (OR 1.68; 95% CI 1.22 to 2.48; $p=0$ .004, Fig. 2).

Development, validation, and performance of a predictive nomogram

In multivariate analysis (Table 1), the radiomics signature and CT-reported LN status were identified as the independent predictors. To provide clinicians with an easy-to-use tool, we generated a radiomics nomogram (Fig. 4). The Hosmer-Lemeshow test yielded nonsignificant p values of 0.528, 0.334 in the training set and the test set, respectively. Therefore, our nomogram suggested a good calibration. The radiomics nomogram performed well in discriminating LN metastasis (+) from LN metastasis (-) in the training set with an AUC of 0.758 (95%CI: 0.681 - 0.836), and showed similar discrimination on internal validation (AUC 0.773; 95%CI: 0.666 - 0.880).

Performance comparison of CT-reported LN status and radiomics nomogram

The AUCs of the CT-reported LN status in the training set and test set were 0.611 (95%CI: 0.537 - 0.685) and 0.586 (95%CI: 0.487 - 0.685), respectively. Notably, the radiomics nomogram achieved considerably better discrimination capability than LN size both in the training set (DeLong's test, $p<0.001$) and in the test set ($p = 0.005$) (Fig. 5).

Incremental predictive value of radiomics signature to CT-reported LN status

Adding radiomics signature to CT-reported LN status significantly improved risk reclassification for LN metastasis both in the training set (IDI 13.7%; 95%CI 8.3% - 19.1%; $p<0.001$; categorical NRI 27.7%; 95%CI 9.4% - 46.0%; $p=0.003$) and in the test set (IDI 17.3%; 95%CI 7.7% - 26.8%; $p<0.001$; categorical NRI 52.3%; 95%CI 22.8% - 81.7%; $p<0.001$).

Clinical usefulness of the radiomics nomogram

By decision curve analysis, the clinical impact of the radiomics nomogram to guide treatment decisions was observed with maximal utility occurring at 0.44. Across the majority of the range of risk thresholds, the radiomics nomogram had the highest net benefit compared with CT-reported LN status and simple strategies such as the "treat none" or "treat all" strategies (Fig. 6).

Discussion

Here we developed and validated a nomogram for the preoperative diagnosis of LN metastasis in patients with resectable ESCC. The radiomics nomogram, which incorporated the radiomics signature and CT-reported LN status, performed

Table 1 Multivariate logistic regression analysis for lymph node metastasis in the training set

Intercept and variable	Multivariate analysis	
	OR (95% CI)	*p*
Intercept	0.451 (0.267 to 0.735)	0.002
Radiomics signature (per 0.1 increase)	1.952 (1.453 to 2.731)	< 0.001
CT-reported LN status	2.158 (1.023 to 4.650)	0.045

Abbreviations: OR, Odds Ratio; 95% CI, 95% confidence interval; CT, computed tomography; LN, lymph node

well in discriminating LN metastasis with an AUC of 0.758 in the training set, and demonstrated similar discrimination on internal validation (AUC 0.773). The comparable discrimination implies that the nomogram was robust in quantifying an individual's risk of LN metastasis. To our knowledge, the current study is the first to explore the predictive value of radiomics for LN metastasis in patients with ESCC, and also the first to compare the predictive performance of a radiomics nomogram and size criteria.

LN metastasis has been widely used to stratify ESCC patients according to the risk of recurrence, which is essential for selection of patients who can benefit from neoadjuvant chemoradiation [22]. Since radiomics can achieve satisfactory discrimination for LN metastasis preoperatively, it may contribute to risk stratification and optimal selection of ESCC patients who require neoadjuvant treatment while avoiding unnecessary treatment for low-risk patients.

Blood-routine derivates including NLR and PLR were deemed to be an important prognostic marker for LN metastasis in esophageal cancer [23]. However, our study indicated the limited value of these two metrics in diagnosis of LN metastasis by either univariate or multivariate analyses. This contradictory result might be attributable to the inherent limitation that the previous studies lack independent validation, which may lead to data overfitting and overestimation. So, NLR and PLR may be not a reliable biomarker for LN metastasis in ESCC.

Although identified as an independent risk factor for LN metastasis in our study, CT-reported LN status alone showed unsatisfactory discrimination (AUC 0.611 in the training set, and AUC 0.586 in the test set). This is in line with several previous reported studies [9, 10, 24]. The efficacy of size criteria (i.e. CT-reported LN status) in the assessment of LN metastasis is still limited.

However, addition of a radiomics signature to CT-reported LN status significantly improved the reclassification performance, both in the training set (IDI 13.7%; $p<0.001$; categorical NRI 27.7%; $p=0.003$) and in the test set (IDI 17.3%; $p<0.001$; categorical NRI 52.3%; $p<0.001$). Therefore, use of the radiomics nomogram can ameliorate the gap that exists between those identified through size criteria alone and the vast majority of undiagnosed LN metastasis of ESCC, which may support the potential use of the radiomics nomogram as a useful tool to help redirect and optimize treatment in this clinical setting.

One possible explanation for radiomics nomogram's superior performance is that radiomics has the potential to decode intratumor heterogeneity on a macroscopic scale noninvasively and quantitatively [11, 13, 15, 25]. The observation that critical genetic events such as ZNF750 mutations, TP53 putative GOF mutations and nucleosome disorganization underlie LN metastasis in ESCC may provide a biological basis for a relationship between tumor heterogeneity and actual LN status [26]. Genetic alterations or instability can lead to different sub-clones with distinct molecular and microenvironmental differences in a malignant lesion, which express different

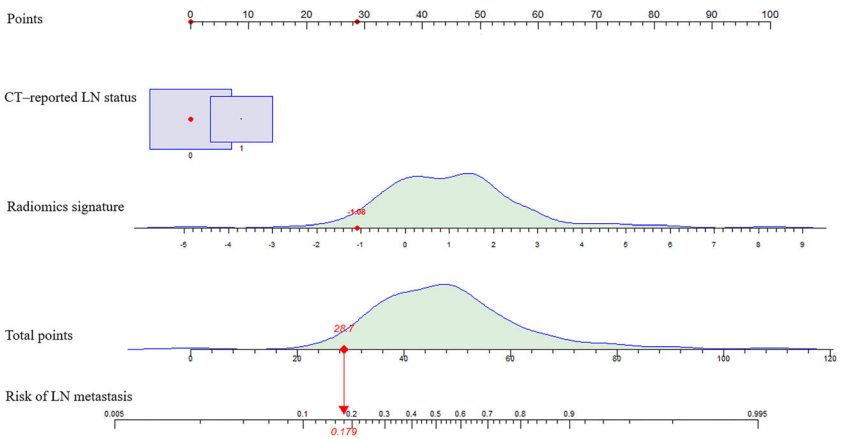

Fig. 4 Developed radiomics nomogram. The distribution of predictors and the total points are superimposed on the nomogram scales. A box plot is presented for showing the distribution of CT–reported LN status, which is a categorical variable. The size of the box represents the proportion a certain category occupied. The density plots show the distribution of continuous variables, such as radiomics signature and total points. In addition, an observation's values are superimposed on the plot, and the exact number of each red spot correspond to each tick mark on that variable's axis. When point scores for individual predictors are added, the total point is 28.7, and the corresponding risk score is as low as 0.179. The patient was pathologically confirmed LN metastasis (-)

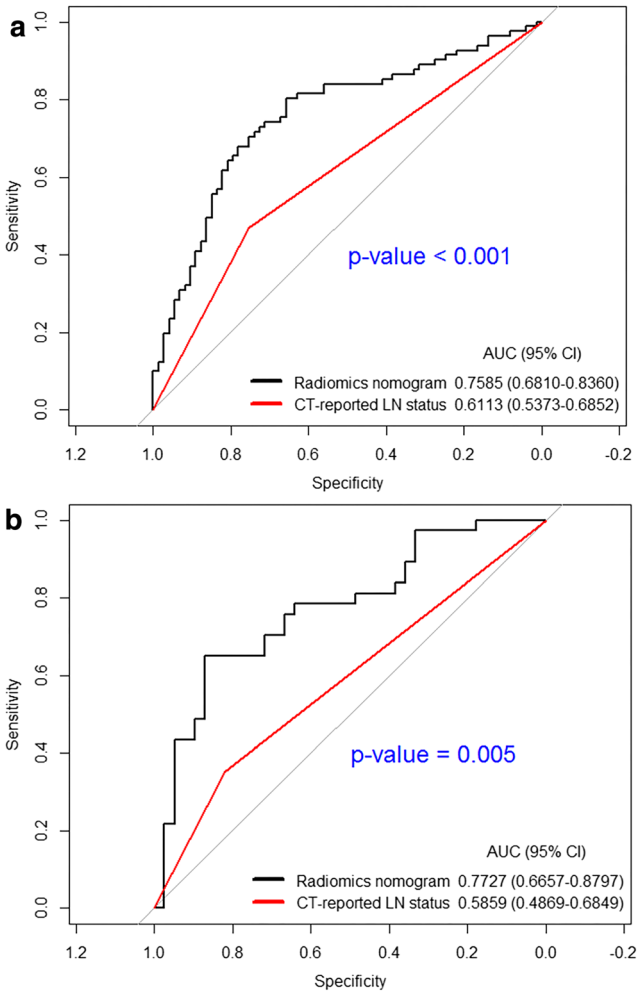

Fig. 5 Receiver operating characteristic (ROC) curves to discriminate LN metastasis (+) from LN metastasis (-) for the radiomics nomogram and the CT-reported LN status. ROC curves for radiomics nomogram had considerably higher area under the ROC curves than those of CT-reported LN status in both the training set (**a**) and the test set (**b**)

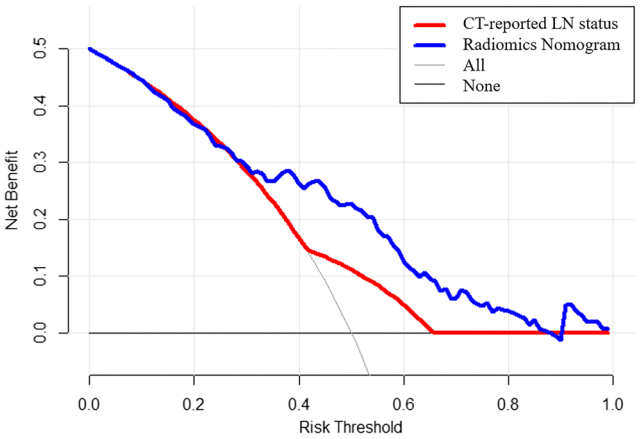

Fig. 6 Net benefit curves for radiomics nomogram compared with CT-reported LN status. The net benefit of using the radiomics nomogram (blue line) for clinical decision-making exceeds that of using CT-reported LN status (red line) across the majority of the range of reasonable risk thresholds

tumor phenotypes (i.e. tumor heterogeneity) such as LN metastatic potential [27]. Although plausible, additional radiogenomic analysis is required to validate this hypothesis in the future.

Although external validation was lacking, the decision curve analysis, which enables the evaluation of clinical impact, suggested that the radiomics nomogram has a higher likelihood of LN metastasis identification than CT-reported LN status. Meanwhile, the radiomics signature added incremental value to CT-reported LN status for individualized estimation across the majority of the range of risk thresholds.

Unlike prior radiomics investigations on LN metastasis that mostly extracted features from the largest cross-sectional area [16, 17], our current study focused on the whole tumor analysis, which takes all the available slices into account, thus providing abundant information about tumor heterogeneity [28]. In addition, we want to point out that tumor necrosis adjacent to lumen was excluded from radiomics analysis in this study. The reasons are as follow: Firstly, just like PET texture analysis in esophageal cancer, only the FDG-avid region of the primary lesion was used as VOI [29, 30]. Obviously, the tumor necrosis adjacent to esophagus lumen with non- or poorly FDG-avid was excluded from texture analysis. In addition, it is very difficult to distinguish tumor necrosis from intraluminal content on CT. Therefore, necrosis adjacent to lumen was excluded to avoid as much as possible the potential influence of intraluminal content on tumor segmentation.

Our study has several limitations. First, only single-center data for both model development and validation were used in this retrospective study. Future work would involve prospective external validation of the nomogram in a large cohort population to generalize the results. Second, we considered only the primary tumor in this study. An integrated radiomics analysis of the primary tumor and lymph nodes may potentially provide higher prediction performance [31] . Third, radiomics is recently reported to be able to probe different gene expressions [32–34] . Therefore, future studies of radiogenomic analysis are desirable for exploring underlying mechanisms of our results.

In conclusion, we constructed a radiomics nomogram that exhibits an excellent discrimination capability in inferring LN status in resectable ESCC. It may serve as a convenient tool for clinicians to estimate individuals' risk of LN metastasis and to guide treatment personalization for those patients, although further multicenter validation is warranted to obtain higher level evidence in subsequent studies.

Funding This study has received funding by the National Key Research and Development Plan of China (grant number: 2017YFC1309100), National Natural Scientific Foundation of China (grant number: 81771912 and U1301258) and Science and Technology Planning Project of Guangdong Province (grant number: 2017B020227012)

Compliance with ethical standards

Guarantor The scientific guarantor of this publication is Changhong Liang.

Conflict of interest The authors of this manuscript declare no relationships with any companies whose products or services may be related to the subject matter of the article.

Statistics and biometry No complex statistical methods were necessary for this paper.

Informed consent Written informed consent was waived by the Institutional Review Board.

Ethical approval Institutional Review Board approval was obtained.

Methodology
- retrospective
- diagnostic or prognostic study
- performed at one institution

References

1. Global Burden of Disease Cancer C, Fitzmaurice C, Allen C et al (2017) Global, regional, and national cancer incidence, mortality, years of life lost, years lived with disability, and disability-adjusted life-years for 32 cancer groups, 1990 to 2015: a systematic analysis for the global burden of disease study. JAMA Oncol 3:524–548
2. Torre LA, Bray F, Siegel RL, Ferlay J, Lortet-Tieulent J, Jemal A (2015) Global cancer statistics, 2012. CA Cancer J Clin 65:87–108
3. Wei WQ, Chen ZF, He YT et al (2015) Long-term follow-up of a community assignment, one-time endoscopic screening study of esophageal cancer in China. J Clin Oncol 33:1951–1957
4. Malhotra GK, Yanala U, Ravipati A, Follet M, Vijayakumar M, Are C (2017) Global trends in esophageal cancer. J Surg Oncol 115: 564–579
5. Zhang HL, Chen LQ, Liu RL et al (2010) The number of lymph node metastases influences survival and International Union Against Cancer tumor-node-metastasis classification for esophageal squamous cell carcinoma. Dis Esophagus 23:53–58
6. Kayani B, Zacharakis E, Ahmed K, Hanna GB (2011) Lymph node metastases and prognosis in oesophageal carcinoma–a systematic review. Eur J Surg Oncol 37:747–753
7. Hong SJ, Kim TJ, Nam KB et al (2014) New TNM staging system for esophageal cancer: what chest radiologists need to know. Radiographics 34:1722–1740
8. van Rossum PS, Xu C, Fried DV, Goense L, Court LE, Lin SH (2016) The emerging field of radiomics in esophageal cancer: current evidence and future potential. Transl Cancer Res 5:410–423
9. Betancourt Cuellar SL, Sabloff B, Carter BW et al (2017) Early clinical esophageal adenocarcinoma (cT1): utility of CT in regional nodal metastasis detection and can the clinical accuracy be improved? Eur J Radiol 88:56–60
10. Foley KG, Christian A, Fielding P, Lewis WG, Roberts SA (2017) Accuracy of contemporary oesophageal cancer lymph node staging with radiological-pathological correlation. Clin Radiol 72: 693.e691–693.e697
11. Sala E, Mema E, Himoto Y et al (2017) Unravelling tumor heterogeneity using next-generation imaging: radiomics, radiogenomics, and habitat imaging. Clin Radiol 72:3–10
12. Yip CS, Davnall F, Kozarski R et al (2013) CT tumoral heterogeneity as a prognostic marker in primary esophageal cancer following neoadjuvant chemotherapy. Pract Radiat Oncol 3:S3
13. Davnall F, Yip CS, Ljungqvist G et al (2012) Assessment of tumor heterogeneity: an emerging imaging tool for clinical practice? Insights Imaging 3:573–589
14. O'Connor JP, Rose CJ, Waterton JC, Carano RA, Parker GJ, Jackson A (2015) Imaging intratumor heterogeneity: role in therapy response, resistance, and clinical outcome. Clin Cancer Res 21: 249–257
15. Gillies RJ, Kinahan PE, Hricak H (2016) Radiomics: images are more than pictures, they are data. Radiology 278:563–577
16. Huang YQ, Liang CH, He L et al (2016) Development and validation of a radiomics nomogram for preoperative prediction of lymph node metastasis in colorectal cancer. J Clin Oncol 34:2157–2164
17. Wu S, Zheng J, Li Y et al (2017) A radiomics nomogram for the preoperative prediction of lymph node metastasis in bladder cancer. Clin Cancer Res 23:6904–6911
18. Rice TW, Gress DM, Patil DT, Hofstetter WL, Kelsen DP, Blackstone EH (2017) Cancer of the esophagus and esophagogastric junction-Major changes in the American Joint Committee on Cancer eighth edition cancer staging manual. CA Cancer J Clin 67:304–317
19. Rice TW, Patil DT, Blackstone EH (2017) 8th edition AJCC/UICC staging of cancers of the esophagus and esophagogastric junction: application to clinical practice. Ann Cardiothorac Surg 6:119–130
20. Umeoka S, Koyama T, Togashi K et al (2006) Esophageal cancer: evaluation with triple-phase dynamic CT–initial experience. Radiology 239:777–783
21. van Griethuysen JJM, Fedorov A, Parmar C et al (2017) Computational radiomics system to decode the radiographic phenotype. Cancer Res 77:e104–e107
22. Medical Research Council Oesophageal Cancer Working G (2002) Surgical resection with or without preoperative chemotherapy in oesophageal cancer: a randomised controlled trial. Lancet 359: 1727–1733
23. Yodying H, Matsuda A, Miyashita M et al (2016) Prognostic significance of neutrophil-to-lymphocyte ratio and platelet-to-lymphocyte ratio in oncologic outcomes of esophageal cancer: a systematic review and meta-analysis. Ann Surg Oncol 23:646–654
24. Luo LN, He LJ, Gao XY et al (2016) Endoscopic ultrasound for preoperative esophageal squamous cell carcinoma: a meta-analysis. PLoS One 11:e0158373
25. Lambin P, Leijenaar RTH, Deist TM et al (2017) Radiomics: the bridge between medical imaging and personalized medicine. Nat Rev Clin Oncol 14:749–762
26. Dai W, Ko JMY, Choi SSA et al (2017) Whole-exome sequencing reveals critical genes underlying metastasis in oesophageal squamous cell carcinoma. J Pathol 242:500–510
27. Burrell RA, McGranahan N, Bartek J, Swanton C (2013) The causes and consequences of genetic heterogeneity in cancer evolution. Nature 501:338–345
28. Ng F, Ganeshan B, Kozarski R, Miles KA, Goh V (2013) Assessment of primary colorectal cancer heterogeneity by using whole-tumor texture analysis: contrast-enhanced CT texture as a biomarker of 5-year survival. Radiology 266:177–184
29. Foley KG, Hills RK, Berthon B et al (2018) Development and validation of a prognostic model incorporating texture analysis derived from standardised segmentation of PET in patients with oesophageal cancer. Eur Radiol 28:428–436

30. Nakajo M, Jinguji M, Nakabeppu Y et al (2017) Texture analysis of (18)F-FDG PET/CT to predict tumor response and prognosis of patients with esophageal cancer treated by chemoradiotherapy. Eur J Nucl Med Mol Imaging 44:206–214
31. Coroller TP, Agrawal V, Huynh E et al (2017) Radiomic-based pathological response prediction from primary tumors and lymph nodes in NSCLC. J Thorac Oncol 12:467–476
32. Aerts HJ, Velazquez ER, Leijenaar RT et al (2014) Decoding tumor phenotype by noninvasive imaging using a quantitative radiomics approach. Nat Commun 5:4006
33. Panth KM, Leijenaar RT, Carvalho S et al (2015) Is there a causal relationship between genetic changes and radiomics-based image features? An in vivo preclinical experiment with doxycycline inducible GADD34 tumor cells. Radiother Oncol 116:462–466
34. Rios Velazquez E, Parmar C, Liu Y et al (2017) Somatic mutations drive distinct imaging phenotypes in lung cancer. Cancer Res 77: 3922–3930